ORIGINAL

Distribution Category UC-90d
DE84001069

CATALYST AND REACTOR DEVELOPMENT FOR A LIQUID PHASE FISCHER-TROPSCH PROCESS

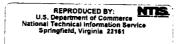
QUARTERLY TECHNICAL PROGRESS REPORT FOR PERIOD 1 JANUARY 1983 - 31 MARCH 1983

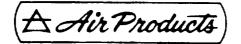
PAUL N. DYER
RONALD PIERANTOZZI
BARRY W. BRIAN
ANDREW F. NORDQUIST
ROBIN L. PARSONS

AIR PRODUCTS AND CHEMICALS, INC.
ALLENTOWN, PA 18105

SEPTEMBER 1983

PREPARED FOR UNITED STATES DEPARTMENT OF ENERGY UNDER CONTRACT NO. DE-AC22-80PC30021





EXECUTIVE SUMMARY

Two major tasks continued in the tenth quarter of the APCI/US DOE contract, "Catalyst and Reactor Development for a Liquid Phase Fischer-Tropsch Process": (1) Slurry Catalyst Development, and (2) Slurry Reactor Design Studies.

The first extended slurry test was continued, using a proprietary catalyst. The results showed that it was possible to produce yields in the diesel fuel region equal to or greater than the Schulz-Flory maximum, without further optimization. Low deactivation rates were observed.

Kinetic rate constants were derived from the CSTR experiments, and used in a computer simulation to predict conversions from bubble column operation under Rheinpreussen conditions.

Short term (21 day) slurry tests were carried out on two other catalysts, optimized by the screening program. Parametric gas phase screening results were concluded for two additional "modified conventional catalysts", and the optimum preparation and activation methods for diesel fuel selectivity were chosen.

In the hydrodynamic studies, work in the 5" column was completed with measurements on the Fe $\frac{0}{3}$ /water slurries.

In the 12" column, fitted with 7 heat transfer tubes, hydrodynamic parameters were determined for slurries of Fe $_{2}$ 0 and 10 and 11 and 12 and 12 and 13 and 14 and 15 and 15

- o Gas holdups were close to the Akita and Yoshida correlation for the hydrocarbon slurries, but lower for the aqueous ones.
- o Solid concentration profiles, modelled by the sedimentation model, gave evidence of particle agglomeration in SiO₂/hydrocarbon slurries, underlining the need to use chemically similar slurries in cold-flow modelling work.

Preceding page blank



- o In the 5" column, solid and liquid dispersion coefficients were found to be equal.
- o Heat transfer coefficients in paraffin slurries in the 12" column were consistently 15-20% below values predicted by Deckwer's correlation.
- o A thermistor and a conical hot film probe were investigated to find the correct combination of sensitivity and robustness for bubble diameter measurement in 3 phase slurries.



TABLE OF CONTENTS

		<u>Pag</u>
1.0	INTRODUCTION	1
2.0	<u>OBJECTIVE</u>	2
3.0	SUMMARY AND CONCLUSIONS	3
	3.1 Task 2 - Slurry Catalyst Development	3
	3.1.1 Sub-Task 2a - Background Studies	3
	3.1.2 Sub-Task 2c - Catalyst Preparatio	on 3
	and Slurry Reactor Tests	
	3.2 Task 3 - Slurry Reactor Design Studies	3
4.0	<u>ACKNOWLEDGEMENTS</u>	. 5
5.0	RESULTS AND DISCUSSION	6
	5.1 Task 2 - Slurry Catalyst Development	6
	5.1.2 Sub-Task 2c - Catalyst Preparatio	n and 6
	Slurry Reactor Tests	
	5.2 Task 3 - Slurry Reactor Design Studies	6
	5.2.1 5" Cold Flow Simulator	6
	5.2.2 12" Cold Flow Simulator	. 9
6.0	EXPERIMENTAL	14
	6.1 Task 2 - Slurry Catalyst Development	14
	6.1.1 Sub-Task 2c - Catalyst Preparation	n and 14
	Slurry Reactor Tests	
	6.2 Task 3 - Slurry Reactor Design Studies	14
7.0	REFERENCES	18
8.0	TABLES	19
9.0	<u>FIGURES</u>	32



LIST OF TABLES

TABLE		PAGE
	5" Cold Flow Simulator, Water/Iron Oxide, Gas Holdup	
1	l-5 μm, particle size	19
2	45-53 μm, particle size	20
3	90-115 μm, particle size	21
4	5" Cold Flow Simulator, Water/Silicon Oxide, Liquid Dispersion	22
	Coefficients	
	12" Cold Flow Simulator, Plain Heat Transfer Internals, Gas	
	Holdup and Solid Fraction	
5	N1trogen/1soparaffin	24
6	Air/water	25
7	Nitrogen/isoparaffin/iron oxide	26
8	Air/water/silicon oxide, air/water/iron oxide	27
	12" Cold Flow Simulator, Plain Heat Transfer Internals,	
	Shell-Side Heat Transfer Coefficients	
9	Nitrogen/isoparaffin	28
10	Air/water	29
11	Nitrogen/isoparaffin/iron oxide	30
12	Air/water/silicon oxide, air/water/iron oxide	31



LIST OF FIGURES

FIGL	<u>IRE</u>	PAGE
	5" Cold Flow Simulator, Water/Iron Oxide, Gas Holdup	
1	0.5-5 µm particle size	32
2	45-53 μm particle size	33
3	90-115 μm particle size	34
	5" Cold Flow Simulator, Water/Iron Oxide, Solid Concentration	
	<u>Profiles</u>	
4	0.5-5 µm particle size	35
5	45-53 µm particle size, part l	36
6	45-53 μm particle size, part 2	37
7	90-106 μm particle size	38
8	5" cold flow simulator, liquid dispersion coefficients, water/	39
	silicon oxide	
	12" Cold Flow Simulator, Gas Holdup, Plain Heat Transfer	
	<u>Internals</u>	
9	Isoparaffin/N ₂	40
10	Water/air	41
11	Iron oxide	42
12	Water/silicon oxide	43
	12" Cold Flow Simulator, Solid Concentration Profiles	
13	Isoparaffin/90-115 µm iron oxide/N ₂	44
14	Water/silicon oxide/air	45
	12" Cold Flow Simulator, Heat Transfer Coefficients,	
	Plain Heat Transfer Internals	
15	Isoparaffin/90-106 µm iron oxide/N ₂	46
16	Water/air	47
17	Water/silicon oxide	48
18.	Bubble Length Distribution Test Problem	49
19	Intermediate Gas Holdup Methods	50



1.0 INTRODUCTION

Coal liquefaction will be an important source of transportation fuels in the future, and can be accomplished by both a direct route (hydrogenation of coal in a donor solvent) or by an indirect route (gasification of coal followed by the Fischer-Tropsch reaction).

The product selectivity of the Fischer-Tropsch reaction has been the focus of extensive research for many years, yet still remains a prime target for technical innovation. Fischer-Tropsch technology, as it is currently practiced commercially for liquid fuels production, provides a broad range of hydrocarbon products which require costly downstream refining.

Selectivity can be influenced by variations in the catalyst composition and process conditions. Yet, in spite of the extensive effort devoted to this problem, a suitable catalyst has not previously been developed for producing a narrow range hydrocarbon product, such as gasoline or diesel fuel, without the coproduction of lighter and heavier undesirable products.

The Fischer-Tropsch reaction is exothermic, and improved heat transfer would also be expected to have a major beneficial effect on product selectivity. Slurry phase reactor operation improves heat transfer and temperature control, and results in greater selectivity to liquid products, usually though lower methane production. However, considerable differences have been reported in the space-time yield, catalyst life and ease of operation of slurry phase reactors.

In addition to improved product selectivity, slurry phase operation offers the advantage of ease of scale-up and the ability to directly utilize the carbon monoxide-rich synthesis gas produced by coal gasifiers. The full potential of the slurry phase Fischer-Tropsch process has not yet been realized, and its further development is an important part in our country's program to establish viable technology for converting coal to hydrocarbon fuels.

Air Products, under contract to DOE, has undertaken a program in catalyst and reactor development for a slurry phase Fischer-Tropsch process, and this report describes the work accomplished during the tenth quarter.

1



2.0 OBJECTIVE

The overall objective of this program is to evaluate catalysts and slurry reactors systems for the selective conversion of synthesis gas into transportation fuels via a single stage, liquid phase process.

Task l - To establish a detailed Project Work Plan. This task was completed in the first quarter.

Task 2 - To evaluate and test catalysts for their potential to convert synthesis gas to gasoline, diesel fuel, or a mixture of transportation fuels suitable for domestic markets, and to quantify catalyst activity, selectivity, stability and aging with a target process concept involving a single stage, liquid phase reactor system.

Task 3 - To evaluate through the use of cold flow reactor simulators, the flow characteristics and behavior of slurry reactors for the production of hydrocarbons from synthesis gas. This includes (1) defining heat, mass and momentum transfer parameters which effect the design of slurry reactors, (2) establishing operating limits for slurry reactors with respect to system physical parameters, (3) developing or confirming correlations for predicting the flow characteristics and heat/mass transfer of slurry reactors, and (4) defining the necessary requirements for the design of larger scale reactors.

Task 4 - To develop a preliminary design for a bench scale slurry phase Fischer-Tropsch reactor.



3.0 SUMMARY AND CONCLUSIONS

3.1 Task 2 - Slurry Catalyst Development

3.1.1 Sub-Task 2a - Background Studies

A computerized survey of available literature and patents dealing with the conventional and slurry phase Fischer-Tropsch processes, and the hydrodynamics of three phase slurry reactors, was continued.

3.1.2 <u>Sub-Task 2c - Catalyst Preparation and Slurry Reactor Testing</u>

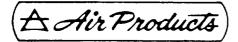
This section contains potentially patentable material and has therefore been issued in a supplementary report marked "Not for Publication".

3.2 Task 3 - Slurry Reactor Design Studies

In the 5" cold flow simulator (CFS), gas holdup and solid concentration measurements were obtained for the <u>water</u>/air/iron oxide systems. These measurements complete the gas holdup studies in the 5" CFS. In the 12" CFS with heat transfer internals, gas holdup and solid concentration profile measurements were obtained for the <u>water</u>/air, <u>isoparaffin</u>/nitrogen, <u>isoparaffin</u>/nitrogen/90-106 µm iron oxide, <u>water</u>/air/silicon oxide, and <u>water</u>/air/0.5-5 µm iron oxide systems. In all of the 5" CFS, and the isoparaffin runs in the 12" CFS, values of gas holdup were close to those predicted by the two phase Akita and Yoshida correlation. Gas holdup in water slurries in the 12" CFS was consistently lower than the Akita and Yoshida correlation.

Solid concentration profiles were modelled using the sedimentation diffusion model of Cova and Kato, and the results gave indication of particle agglomeration in the isoparaffin/silicon oxide systems.

Liquid dispersion measurements were analyzed for most of the zero slurry velocity runs, and the dispersion coefficients were in agreement with the same Kato correlation. Therefore liquid and solid dispersion coefficients were found to be equal in the 5" CFS.



Heat transfer coefficients were determined in the 12" CFS. Tests performed in isoparaffin gave coefficients that were consistently 15-20% below those values predicted by Deckwer. Values obtained in aqueous slurries were consistently lower than predicted.

In the bubble diameter measurement program, an improved integration convergence routine was written to analyze the measured bubble cord lengths. However, difficulties were experienced with the bubble diameter probe which did not have sufficient mechanical strength in the three phase system. Several alternatives, including a thermistor probe and a conical hot film probe, were investigated.



4.0 ACKNOWLEDGEMENTS

The contributions made to this program by P. A. Greene, J. M. LaBar, M. Louie, S. E. Madison, S. Motika and L. E. Schaffer are gratefully acknowledged.



5.0 RESULTS AND DISCUSSION

5.1 Task 2 - Slurry Catalyst Development

5.1.2 <u>Sub-Task 2c - Catalyst Preparations and Slurry Reactor Tests</u>

This section contains potentially patentable material and has therefore been issued in a supplementary report marked "Not for Publication".

5.2 Task 3 - Slurry Reactor Design Studies

5.2.1 5" Cold Flow Simulator

(1) Gas Holdup

Gas holdup measurements were obtained for the water/air/iron oxide systems, and are shown in Tables 1-3 and Figures 1-3 for the 0.5-5, 45-53, and 90-106 µm particle sizes, respectively. Gas holdups were similar to those found using isoparaffin as the liquid, falling between the Pilhofer and Bach (3) and Akita and Yoshida (1) correlations. Compared with the water/silicon oxide system, the iron oxide gas holdups were higher. The effect of particle size and slurry velocity on gas holdup appears negligible. These measurements complete the gas holdup studies in the 5" cold flow simulator. Statistical analysis will subsequently be performed.

(11) Solid Concentration Profiles

Solid concentration profiles are shown in Figure 4 for the $0.5\text{--}5~\mu\text{m}$, in Figures 5 and 6 for the $45\text{--}53~\mu\text{m}$, and in Figure 7 for the $90\text{--}106~\mu\text{m}$ iron oxide/water system. The concentration profiles are slightly less pronounced or equal to those observed in the isoparaffin/iron oxide system, as solid/liquid density differences would predict. As found previously, the most pronounced profiles were observed for the $90\text{--}106~\mu\text{m}$ iron oxide runs at zero liquid velocity. These measurements complete the acquisition of solid dispersion data in the 5" CFS.

An attempt was made to model the solid concentration profiles determined to date, using the sedimentation diffusion model of Cova (4) and Kato (5). For continuous flow of both gas and slurry, the sedimentation diffusion model gives:

$$C_2 = \left[C_H/(V_L - V_{ST})\right]\left(V_L - V_{ST} \exp\left[(V_L - V_{ST})(Z_2 - L)/E_{ZS}\right]\right)$$
(1)

For batch operation with $V_i = 0$,

$$c_2 = c_1 \exp \frac{-v_{ST}}{E_{ZS}} (Z_2 - Z_1)$$
 (2)

These analytical expressions result from the assumption that solid settling, due to the density difference between solid and liquid, is superimposed upon the tendency for the gas phase to suspend the catalyst particles. There are three parameters in eqn. (1) which must be determined:

 ${
m C}_{
m H}$ - the solid concentration at the top of the expanded bed, ${
m V}_{
m ST}$ - the average settling velocity of the solid particles,

E_{ZS} - the solid phase axial dispersion coefficient

 C_H has empirically been found to be approximately 25-30% higher than the feed concentration (5). E_{ZS} was found to agree closely with the empirical correlation of Kato (5), which is the same equation that is used to describe the extent of axial dispersion of the liquid phase (see following section). Values of V_{ST} were variable, however. If the assumption is made that there is no surface interaction between the solid and liquid phases, then, for particles diameters <50 μ m, the following expression can be theoretically derived for a particle settling in a slurry:

(A Air Products)

$$V_{ST, CALC} = g d_S^2 (\rho_S - \rho_{SL})/(18 \mu_{SL} (1 + F_S \rho_L / F_L \rho_S))$$
 (3)

However, solid/liquid interactions were observed. For the silicon oxide/isoparaffin system, a larger measured $V_{\rm ST}$ than predicted by Eqn. (3) indicated that particle agglomeration occurred in the slurry. Conversely, the iron oxide/isoparaffin system showed higher concentrations in the middle of the column than immediately above the distributor, possibly suggesting a solid/gas affinity. This type of interaction illustrates the limitations of the sedimentation diffusion model in predicting solid dispersion in the CFS results. The results of this work have been reported (6).

(111) Liquid Dispersion

Liquid dispersion measurements were made in all aqueous runs in the 5" cold flow simulator. Many of those at zero slurry velocity are included in Table 4 and Figure 8. The measured dispersion coefficients are on average, close to but lower than those predicted by Kato, et al. (5).

$$Pe = \frac{13 F_r}{1 + 8 F_r^{0.85}}$$
 (4)

where

$$Pe = dp V_G/E_{ZL}$$
 (5)

$$F_r = V_6 \sqrt{g \, dp} \tag{6}$$

This difference can probably be attributed to the differing sampling methods used. Whereas in this work, conductivity measurements were made in situ, Kato's measurements were at the outlet. Some additional diffusion may have occurred as a result. In situ measurements have the inherent disadvantage of added scatter due to bubble impingement on the conductivity probe, which may account for the scatter in Figure 8. Particle size, in this system, appears to have little effect on liquid dispersion.



5.2.2 12" Cold Flow Simulator

(1) Gas Holdup

In order to develop a relationship between existing two phase correlations and this work, gas holdup measurements were obtained for the two phase isoparaffin/nitrogen and water/air systems, both with heat transfer internals. These are shown in Tables 5 and 6 and Figures 9 and 10, respectively.

The isoparaffin data falls between the Akita and Yoshida (1) and Pilhofer and Bach (3) correlations, while the water/air gas holdups are below the Akita and Yoshida (1) correlation. These results are consistent with those obtained without heat transfer internals, as reported in the July-September 1982 Quarterly Report. Part of the difference may be accounted for by the increased surface tension of the water/air system, although the greater density of water would tend to increase gas holdups. However, these results indicate that internals have little or no effect on gas holdup when correlated against superficial linear gas velocity, accounting for the reduction in column cross sectional area.

Gas holdup measurements were also obtained with heat transfer internals for the isoparaffin/90-106 μm iron oxide, water/silicon oxide, and water/0.5-5 μm iron oxide systems, and these are shown in Tables 7 and 8, and Figures 11 and 12, respectively. The water/0.5-5 μm iron oxide system required only a single measurement to satisfy the experimental design, and this is also plotted in Figure 11.

The addition of solids tends to reduce the gas holdup in isoparaffin to the Akita and Yoshida correlation whether the solid is iron oxide, as reported here or silicon oxide, as reported in the October-December 1982 Quarterly Report. This may be due to an increase in viscosity associated with an increase in weight loading. The water/silicon oxide system does not tend to show this effect on gas holdup. The lower gas holdups at the bottom

section of the column could be partly attributed to solid settling. There also appears to be a slight effect of distributor hole size on gas holdup in the lower section of the column.

(11) Solid Concentration Profiles

Solid concentration profiles are also shown in Tables 7-8 and Figures 13 and 14. As previously observed in the 5" CFS, silicon oxide is better suspended in water than in isoparaffin. The 0.5-5 µm iron oxide remains uniformly suspended, as expected.

The considerable settling observed at the base of the column for the isoparaffin/90-106 µm system, shown in Figure 13, indicated that the maximum weight percent of suspendable solids was exceeded. Due to the difficulty in measuring the high slurry weight percent, runs 47 and 48 were assumed to be at 80 weight percent at sample port #1 when calculating average weight loading. This overestimates the average suspended solids by about 10 wt%.

These results also agree directionally with the sedimentation diffusion model.

(111) Heat Transfer

Heat transfer measurements were made for the two phase isoparaffin/nitrogen and water/air systems, and for the three phase isoparaffin/90-115 μm iron oxide, water/silicon oxide, and water/0.5-5 μm iron oxide systems. These are shown in Tables 9-12, respectively and in Figures 15-17.

For each run, three heat transfer coefficients are reported. Heater A is located inside the center heat transfer internal about 10' above the distributor plate, or about 2/3 of the distance between the distributor and the top of the bubble column. Two temperatures are measured at the heater midpoint, 150° circumferentially from each other. Heater C, 5' above the distributor, is located on one of the six outer tubes with the surface thermocouple oriented toward the column center. The results continue to indicate no detectable circumferential effect on heat transfer coefficient. For two-phase heat transfer

measurements, the slurry properties used in the Deckwer correlation (7) simplify to liquid phase properties. For the isoparaffin runs (see Figure 15), the observed results are consistently 16-19% below those predicted by the Deckwer correlation.

Heat transfer measurements were made for the water systems, (see Figures 16 and 17). These showed much more variation between heaters than previously determined, suggesting the possibility of a partial short circuit. A check of the heater's electrical system for leakage showed them to be operating correctly. These results are contrary to the isoparaffin runs which agreed more closely with the Deckwer (7) correlation and showed no appreciable variations between heaters.

Other measurements will be made in aqueous slurries at different gas velocities to try to elucidate the reasons for this difference.

(1v) Bubble Diameter

An improved convergence and integration routine was written for the program supplied by Dennis Smith of PETC to allow for convergence of the two parameter generalized gamma distribution. A test problem using bubble size data supplied by PETC was then successfully run, giving a=-1.776 and n=-0.2941 to the cumulative distribution function.

$$CZ(\lambda) = \frac{\int_{0}^{\lambda_{Y}} \int_{Y}^{\infty} x^{n-1} e^{aX} dx dY}{\int_{0}^{\infty} Y \int_{Y}^{\infty} x^{n-1} e^{aX} dx dY}$$
(7)

where

 $CZ(\lambda)$ = probability of observing a bubble cord length less than

λ = signal length, cm

X. Y = variables of integration

Figure 18 shows a comparison of the observed versus calculated gamma distribution function.

The above distribution is only for the measured bubble chord lengths. To relate this to a distribution of bubble diameters, the analysis of Tsutsui and Miyauchi (8) will be used:

$$\chi(D_{b}) = \begin{bmatrix} \frac{dZ(\lambda)/\lambda}{d\lambda} \\ \int_{0}^{\infty} -\frac{d(Z(\lambda)/\lambda)}{d\lambda} d\lambda \end{bmatrix}$$
(8)

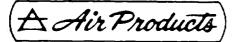
where

 $X(D_b)$ = probability that a bubble has a bubble diameter, D_b $Z(\lambda)$ = probability that the probe has observed a bubble chord length, λ

Difficulties were experienced with the hot film probe. The probe was left in water for ten days while the calibration procedure was being developed. By the end of that time, the soldered wires to both sensors had separated from the probe. Analysis of the probe by the vendor revealed corrosion at the solder joints, possibly due to incomplete quartz coating of the wire and support. Meanwhile, a replacement probe was used for the calibration. However, its wire, too, soon separated from the probe.

A third probe utilized for testing in the slurry separated after 1-2 days of operation in the 12" cold flow simulator. A fourth probe provided by the vendor, with a thicker coating to resist the corrosive and errosive environment of the slurry, lasted one day in the 12" CFS.

At this point, it was concluded that the quartz coated, hot wire probe did not have the necessary mechanical robustness. An alternative thermistor probe, encased in a 24 gauge hypodermic needle, was therefore obtained from the vendor. While its principle of operation is very similar to



the hot wire probe, the sensing element is in the form of a tip instead of wire strung between two supports. Four days of subjecting the thermistor probe to a water slurry showed no change in the probe's resistance, indicating that mechanical integrity was maintained. At the same time, existing electronics were changed to make them compatible with the thermistor probe. In operation, the thermistor probe is given a sufficient current to cause it to heat up slightly. Liquid and gas passing by the probe cool it down at different rates, causing the probe to equilibrate at different temperatures for each phase. Each different temperature corresponds to a unique resistance and voltage (applying a constant current), which is detected by the electronics.

While a response was obtained from the thermistor probe, the electronics did not appear to have the required sensitivity to detect individual bubbles. Therefore, a more sensitive, Honeywell Accudata 218 amplifier, was modified to record the thermistor probe's response.

Subsequently, a conical tipped hot film probe was found to have both the necessary rapid response time and mechanical rigidity to withstand the errosive environment of the three phase slurry.



6.0 <u>EXPERIMENTAL</u>

6.1 Task 2 - Slurry Catalyst Development

6.1.1 <u>Sub-Task 2c - Catalyst Preparation and Slurry Reactor Tests</u>

This section contains potentially patentable material and has therefore been issued in a supplementary report marked "Not for Publication".

6.2 <u>Task 3 - Slurry Reactor Design Studies</u>

(1) Gas Holdup Measurements Using Manometer Tubes

Intermediate gas holdup measurements can be obtained by measuring the pressure drop between two axial points along the bubble column. The several methods used to date, all using manometer tubes, are described as follows:

(a) Method 1 - Bubble Column Liquid

The first method, used successfully in the 5" CFS (see Figure 19.1) used the same liquid in the manometer tube as in the bubble column, with those liquids in intimate contact. The resulting expression

$$\epsilon_{G} = 1 - \frac{HS(TA - TD + (D - A))}{TA(0) - TO(A)}$$
 (9)

gave accurate average gas holdup values between the two manometer tube ports. Difficulties were encountered in applying this method to the 12" column for most of the slurry runs, because the manometer tubes were not tall enough to accommodate the necessary height. For example, with a typical slurry specific gravity of 1.5, the height of the lowest manometer tube would need to be twice as high as the column in order to obtain a reading.

It is important in employing this method that no solid enters the manometer tube from the column. Therefore, before the measurements were made, the tubes were filled with column liquid, ensuring that when the valve between the tube and column was opened, liquid would always flow into the column.

(b) <u>Method 2 - Mercury Manometers</u>

Since the existing manometer tubes did not have sufficient height, mercury manometer tubes (see Figure 19.2) were used instead. The equation for calculating gas holdup then becomes:

$$\epsilon_{G} = 1 - \frac{HS(L - G)}{A - D(G)} \tag{10}$$

where

$$G = \frac{g(TA)\rho_{Hg} - P_1}{g(TD)\rho_{HG} - P_1}$$

This method is not as accurate as Method i, since the pressure above the expanded slurry needs to be subtracted from the mercury readings.

(c) <u>Method 3 - Mercury Manometers Connected to Vapor Space</u> <u>Above Slurry</u>

The inaccuracy of Method 2 can be overcome by connecting one arm of the mercury manometer tubes to the vapor space above the slurry, (see Figure 19.3). Equation (2) then simplifies to

$$\varepsilon_{G} = 1 - \frac{HS(TA - TD)}{TA(D) - TD(A)}$$
 (11)

Near the top of the column, the mercury height, TD, became so small that a manometer tube filled with isoparaffin was used instead. In this case, it was necessary to retain the densities of the manometer liquid in the equation.

$$\varepsilon_{G} = 1 - \frac{HS \left(TA_{PHg} - TD_{PISO}\right)}{TA_{PHg}D - TD_{PISO}A}$$
(12)

In Methods 2 and 3, it is important that only gas be between the column top and the mercury. Therefore, a nitrogen purge was used to return any buildup in the lines back to the column. All of the methods assume $\rho_{\rm G} << \rho_{\rm L}$.

<u>Nomenclature</u>

A	distance above distributor to lower manometer tap, cm
С	concentration, g/cm ³
D	distance above distributor to higher manometer tap, cm
d	diameter, cm
Ez	dispersion coefficient in the Z-direction, cm ² /s
Fr	V _G g d _C Froude number
H _s	Settled, unaerated bed height, cm
g	gravitational acceleration constant, cm/s ²
L	column length, cm
Pe	V _G d _C /E ₇ Peclet number
Re _D	$V_{p}d_{S}\rho_{1}/\mu_{1}$ Particle Reynolds number based on liquid properties
	$V_{ST}d_{S}\rho_{SL}/\mu_{SL}$ Particle Reynolds number based on slurry properties
TA	liquid height in lower manometer tube, cm
TD .	liquid height in higher manometer tube, cm
V	velocity, cm/sec
Z	distance above distributor, cm

igtriangledown igtriangl

Greek Letters

e volume fraction, holdup

ρ density, g/cm³

μ viscosity, g/cm·sec

Subscripts

C column

CALC calculated

G gas

H top of column

ISO isoparaffin

L liquid

P particle

S solld

SL slurry

ST particle in slurry

ZL in Z-direction of liquid

ZS in Z-direction of solid

at a position in the column, higher than point 2

at a position in the column, higher than point 1

7.0 REFERENCES

- 1. K. Akita. and F. Yoshida, <u>Ind. Eng. Chem. Proc. Des. Dev.</u>, 1973, 12, 76.
- 2. H. Hikita and Kikukawa, Chem. Eng. J., 1973, 81, 74.
- 3. T. H. Pilhofer, H. F. Bach and K. H. Mangartz, <u>ACS Symp. Ser.</u>, 1978, 65, 372.
- 4. D. R. Cova, <u>Ind. and Eng. Chem. Proc. Des. and Dev.</u>, 1966, <u>5</u>, 20.
- 5. Y. Kato, A. Nishiwaki, T. Fukuda and S. Tanaka, <u>Chem. Eng. of</u>
 <u>Japan</u>, 1972, <u>5</u>, 112.
- 6. B. W. Brian, and P. N. Dyer, <u>The Effect of Gas and Liquid</u>

 <u>Velocities and Solid Size on Solid Suspension in a Three Phase</u>

 <u>Bubble Column Reactor</u>, presented at the 185th ACS National Meeting, March 1983.
- 7. W.-D. Deckwer, et al., <u>Ind. Eng. Chem. Proc. Des. Dev.</u>, <u>1980</u>, 19, 699.
- 8. T. Tsutsui, and T. Miyauchi, <u>Intil. Chem. Eng.</u>, 1980, 20, 3, 386.

TABLE 1

GAS HOLDUP: 5" COLD FLOW SIMULATOR

SYSTEM: THREE PHASE

GAS- AIR

LIQUID- WATER

SOLID- 1-5 µM IRON OXIDE

RUN	VG FT/SEC	VL FT/SEC	EG EXP	EG23 EXP	EG34 EXP	EG45 EXP	WEIGHT FRACTION
7258-41-1	0.294	0.050	0.196	0.161	0.239	0. 200	0.101
7258-42-1	0.240	0.050	0.164	0.167	0.167	0.172	0.177
7258-43-1	0.290	0.0	0.210	0.159	0.159	0.159	0.187
725°-44-1	0.290	0.100	0.231	0.254	0.254	0.238	0.186
7258-45-1	0.526	0.050	0.204	0.242	0.186	0.180	0.184
7258-46-1	0.290	0.050	0.154	0.159	0.134	0.155	0.278

TABLE 2

GAS HOLDUP: 5" COLD FLOW SIMULATOR

SYSTEM: THREE PHASE

GAS- AIR

LIQUID- WATER

SOLID- 45-53 µM IRON OXIDE

RUN	VG FT/SEC	VL FT/SEC	EG EXP	EG23 EXP	EG34 EXP	EG45 EXP	WEIGHT FRACTION
7258-47-1	0.164	0.050	0.181	0.175	0.254	0.151	0.091
7258-48-1	0.292	0.0	0.167	0.144	0.171	0.168	0.107
7258-49-1	0.298	0.100	0.346	0.423	0.391	0.315	0.105
7258-50-1	0.290	0.090	0.175	0.207	0.163	0.157	0.100
7258-51-1	0.540	0.050	0.196	0.181	0.181	0.177	0.083
7258-52-1	0.168	0.0	0.105	0.064	0.078	0.106	0.152
7258-53-1	0.290	0.050	0.182	0.165	0.139	0.175	0.188
7258-54-1	0.288	0.050	0.185	0.161	0.135	0.171	0.193
7258-55-1	0.288	0.050	0.183	0.168	0.124	0.177	0.189
7258-56-1	0.172	0.110	0.079	0.094	0.067	0.082	0.154
7258-57-1	0.490	0.090	0.188	0.187	0.172	0.181	0.184
7258-58-1	0.500	0.0	0.258	0.199	0.233	0.241	0.174
7258-59-1	0.282	0.0	0.160	0.128	0.116	0.147	0.261
7258-60-1	0.282	0.090	0.183	0.167	0.180	0.170	0.193
7258-61-1	0.470	0.060	0.246	0.229	0.229	0.226	0.190
7258-62-1	0.174	0.060	0.108	0.112	0.098	0.104	0.137

TABLE 3
GAS HOLDUP: 5" COLD FLOW SIMULATOR

SYSTEM: THREE PHASE

GAS- AIR

LIQUID- WATER

SOLID- 90-115 µM IRON OXIDE

RUN	VG FT/SEC	VL FT/SEC	EG EXP	EG23 EXP	EG34 EXP	EG45 EXP	WEIGHT FRACTION
7258-63-1	0.284	0.050	0.169	0.142	0.264	0.159	0.093
7258-64-1	0.500	0.050	0.242	0.203	0.203	0.212	0.226
7258-65-1	0.290	0.0	0.173	0.137	0.161	0.163	0.223
7258-66-1	0.166	0.060	0.121	0.095	0.082	0.120	0.201
7258-67-1	0.276	0.110	0.158	0.159	0.159	0.155	0.177
7258-68-1	0.272	0.050	0.167	0.112	0.124	0.150	0.280
7258-70-1	0.200	0.0	0.133	•	•	•	0.165
7258-71-1	0.500	0.0	0.234	•	•	•	0.165

TABLE 4 ...
LIQUID DISPERSION COEFFICIENTS: 5" COLD FLOW SIMULATOR

SYSTEM: THREE PHASE

GAS- AIR

LIOUID- WATER

RUN NO.	SULID SIZE AVG	LID - SILICON VELOCITY SLURRY GAS FT/SEC	C 71
6962-78	2.50 21.5	0.0 0.05	200.0 131.9
6962-79	2.50 20.8	0.0 0.13	200.0 158.1
6962-80	2.50 18.8	0.0 0.22	180.0 183.7
6962-81	2.50 19.8	0.0 0.35	180.0 217.4
6962-82	2.50 19.5	0.0 0.50	200.0 253.1
6962-83	2.50 11.3	0.0 0.05	135.0 131.9
6962-84	2.50 11.1	0.0 0.10	125.0 148.8
6962-85	2.50 11.3	0.0 0.20	140.0 178.3
5962-86	2.50 11.2	0.0 0.35	170.0 217.4
6962-87	2.50 10.8	0.0 0.50	180.0 253.1
6962-83	98.00 22.0	0.0 0.10	135.0 148.8
6962-89	98.00 23.6	0.0 0.20	160.0 178.3
6962-90	98.00 24.6	0.0 0.30	130.0 204.8